IEEE Photonics Journal
An IEEE Photonics Society Publication

Open Access

Analysis and Optimization of Hybrid Plasmonic Waveguide as a Platform for Biosensing

Volume 6, Number 4, August 2014

M. Z. Alam
F. Bahrami, Student Member, IEEE
J. S. Aitchison, Member, IEEE
M. Mojahedi, Member, IEEE

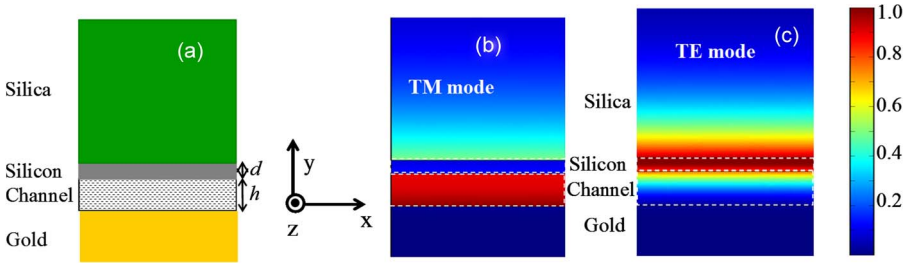

DOI: 10.1109/JPHOT.2014.2331232
1943-0655 © 2014 IEEE

IEEE photonics SOCIETY

IEEE

Analysis and Optimization of Hybrid Plasmonic Waveguide as a Platform for Biosensing

M. Z. Alam, F. Bahrami, *Student Member IEEE*, J. S. Aitchison, *Member*, *IEEE*, and M. Mojahedi, *Member*, *IEEE*

Department of Electrical and Computer Engineering, University of Toronto, Toronto, ON M5S 3G4, Canada

DOI: 10.1109/JPHOT.2014.2331232

Manuscript received May 15, 2014; accepted May 30, 2014. Date of publication June 18, 2014; date of current version June 30, 2014. This work was supported in part by the Natural Sciences and Engineering Research Council of Canada under Grant 480586 and in part by BiopSys Network under Grant 486537. Corresponding author: M. Z. Alam (e-mail: muhammad.alam@mail.utoronto.ca).

Abstract: Hybrid plasmonic waveguides (HPWGs) have received attention worldwide for many different kinds of applications, including on-chip polarization control, enhanced nonlinear optical effects, and biosensing. The HPWG sensor can achieve detection limit lower than possible with purely plasmonic sensors. It can be also used for obtaining additional information about complex biological samples. We analyze the effects of various parameters on such a sensor, optimize the sensor design, and predict the optimum performance achievable for an HPWG sensor in the Mach–Zehnder configuration. We also compare the performance of the HPWG sensor to those of other plasmonic sensors.

Index Terms: Surface plasmon, biosensor.

1. Introduction

Hybrid plasmonic waveguides (HPWGs) have attracted a lot of interest from the plasmonics research community in last few years [1]–[10]. Many different applications of the HPWG have been suggested for optical communication systems [4]–[6]. The HPWG can also be used to implement biosensors, which are compact [7], highly sensitive [8] and can provide more information about a sample than is possible by purely plasmonic sensors [9], [10]. Although a significant amount of work on HPWG sensors has been reported, many important questions remain unanswered. For example, most of the previously reported HPWG sensors were designed using silicon as the high index material and the wavelength of operation was chosen to be 1.55 μm [7]–[9]. No analysis has been carried out to date to confirm whether these choices are optimum. The highest sensitivity expected from such sensors is also yet to be reported. In this paper, we analyze the HPWG sensor to answer the questions mentioned above. The paper is organized as follows. In Section 2, we review the principle of operation of HPWG sensors, and also discuss the potential advantages of such sensors over purely plasmonic alternatives. In Section 3, we investigate the effects of waveguide dimensions and wavelength on the sensor performance. From this analysis we observe that the effects of various parameters on the HPWG sensor performance are rather complicated and a detailed numerical analysis is necessary to find the optimum HPWG sensor design. We carry out this analysis and present the summary of the results

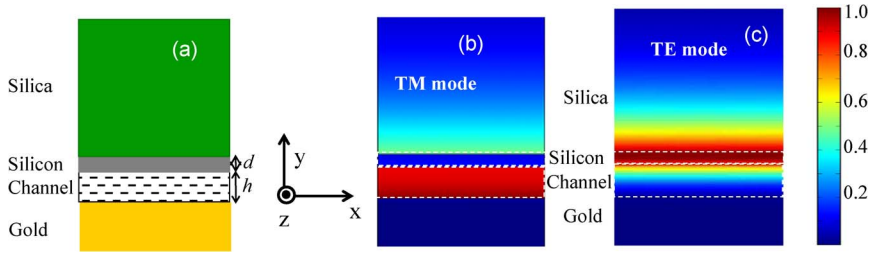

Fig. 1. (a) Schematic of HPWG. Coordinate system used in this work is also shown. (b) and (c) Guided power densities for the TM mode and the TE mode, respectively. Waveguide dimensions are $h = 100$ nm and $d = 50$ nm. Wavelength of operation is 1.55 μm.

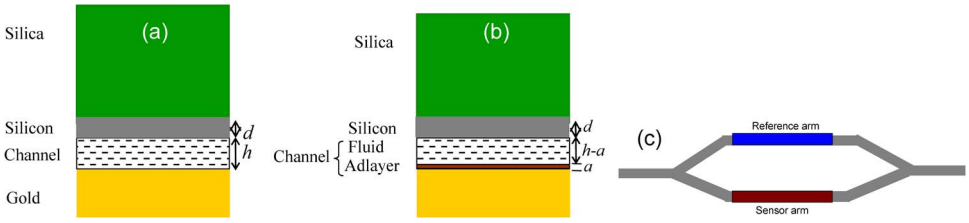

Fig. 2. (a) HPWG waveguide when molecules to be detected is absent in the sample filling the channel. (b) HPWG waveguide when the molecules to be detected are present in the sample and an adlayer is formed on the metal surface. (c) HPWG sensor in the MZI configuration.

in the same section. Section 4 concludes the paper with a discussion of the results presented in previous sections.

2. Principle of Operation and Potential Advantages of the HPWG Biosensor

The HPWG is formed by separating a high index medium from a metal plane by a low index spacer. For example, as shown in Fig. 1(a), the hybrid structure can be formed by separating a gold surface from a silicon slab by a nano-fluidic channel. Typical power distributions for the transverse magnetic (TM) and transverse electric (TE) modes for this structure are shown in Fig. 1(b) and (c), with the interface of the various layers marked by dashed white lines. As shown by the coordinate system in the figure, the metal-channel interface is along the xz interface. Properties of the various materials are taken from [11], [12] for these simulations.

If the metal surface is functionalized for the detection of a specific biomolecule, in the absence of those molecules the channel will be filled with only by a liquid [Fig. 2(a)] but when the molecules to be detected are present in the biological sample, they will attach to the metal surface, and form an adlayer of thickness a as shown schematically in Fig. 2(b). As seen from Fig. 1(b) and (c), the nano-fluidic channel has very high power confinement for the TM mode, and also has significant power confinement for the TE mode. Therefore the presence of adlayer would significantly affect the guided mode, and the HPWG waveguide can be used as a biosensor. The HPWG biosensor can be implemented in many different configurations; for example using a Mach-Zehnder interferometer (MZI), prism coupling or by using grating. For this analysis we chose to investigate HPWG sensor in the MZI configuration because of its high sensitivity, and compatibility with planar technology. As shown in Fig. 2(c), such a device consists of a sensing HPWG arm which is typically coated with binding molecules and a reference arm which is coated with some material that inhibits adsorption on the surface.

Since the HPWG closely resembles a surface plasmon (SP) based sensors, it is important to discuss the potential benefits of this structure compared to the purely plasmonic sensor. Although the field of plasmonics has established itself as a highly successful, label free biosensing technology, plasmonic sensors suffer from a number of limitations [13]. They usually cannot determine both adlayer thickness and index and therefore, one of these quantities needs to be

known or assumed. It is also difficult to differentiate between the changes of bulk index and adlayer thickness using a plasmonic sensor. A sensor that can retain the advantages of SP sensing and can obtain more information about the sample or achieve a lower limit of detection (LoD) will be useful for many applications. In the following we will explain how HPWG sensors can be used to achieve some of these objectives.

Propagation constant of the guided mode is defined as:

$y = \beta + j\alpha$; γ is the propagation constant of the guided mode, α and β are the attenuation and phase constants, respectively;

$N_{\text{eff}} = \gamma/\beta_0 = n_{\text{eff}} + jk_{\text{eff}}$; N_{eff} is the effective mode index; β_0 is free space wave number and n_{eff} and k_{eff} are real and imaginary parts of the effective mode index;

$a =$ adlayer thickness;

$n_c =$ refractive index of the bulk solution.

When there is a change of adlayer thickness the effective index of the guided mode is changed. The change of effective index caused by unit change in adlayer thickness is known as surface sensitivity, which means

$$\frac{\partial n_{\text{eff}}}{\partial a} = \text{surface sensitivity}.$$

Similarly, the change of effective index for a unit change in bulk index is known as bulk sensitivity

$$\frac{\partial n_{\text{eff}}}{\partial n_c} = \text{bulk sensitivity}.$$

In this work, the nature of the mode (TE or TM) will be noted with the symbol where there is a risk of ambiguity. For example, $n_{\text{eff}}(\text{TM})$ will mean the real part of the effective mode index of the TM mode and $\partial n_{\text{eff}}/\partial a$ (TE) would mean the surface sensitivity of the TE mode. If the bulk index and adlayer thickness change by amount Δn_c and Δa, and the resulting change in effective mode index for the TE mode is $\Delta N(\text{TE})$, we can relate these quantities using the concepts of surface and bulk sensitivities

$$\Delta N(\text{TE}) = \frac{\partial n_{\text{eff}}}{\partial n_c}(\text{TE})\Delta n_c + \frac{\partial n_{\text{eff}}}{\partial a}(\text{TE})\Delta a. \tag{1}$$

Similarly for the TM mode, we can write

$$\Delta N(\text{TM}) = \frac{\partial n_{\text{eff}}}{\partial n_c}(\text{TM})\Delta n_c + \frac{\partial n_{\text{eff}}}{\partial a}(\text{TM})\Delta a. \tag{2}$$

Rearranging (1) and (2), we can find the expressions to calculate Δn_c and Δa from measured $\Delta N(\text{TE})$ and $\Delta N(\text{TM})$ using the following relations [14]

$$\Delta n_c = \frac{1}{\frac{\partial n_{\text{eff}}}{\partial n_c}(\text{TE})\frac{\partial n_{\text{eff}}}{\partial a}(\text{TM}) - \frac{\partial n_{\text{eff}}}{\partial a}(\text{TE})\frac{\partial n_{\text{eff}}}{\partial n_c}(\text{TM})}\left[\frac{\partial n_{\text{eff}}}{\partial a}(\text{TM})\Delta N(\text{TE}) - \frac{\partial n_{\text{eff}}}{\partial a}(\text{TE})\Delta N(\text{TM})\right] \tag{3}$$

$$\Delta a = \frac{1}{\frac{\partial n_{\text{eff}}}{\partial n_c}(\text{TE})\frac{\partial n_{\text{eff}}}{\partial a}(\text{TM}) - \frac{\partial n_{\text{eff}}}{\partial a}(\text{TE})\frac{\partial n_{\text{eff}}}{\partial n_c}(\text{TM})}\left[-\frac{\partial n_{\text{eff}}}{\partial n_c}(\text{TM})\Delta N(\text{TE}) + \frac{\partial n_{\text{eff}}}{\partial n_c}(\text{TE})\Delta N(\text{TM})\right]. \tag{4}$$

Carrying out a procedure similar to the one described above, it is also possible to determine both adlayer index and thickness when the bulk index is known. Because of the polarization diversity, the HPWG sensor can also be used to find additional structural information about anisotropic molecules, similar to dual polarization interferometer [13]. As shown in Fig. 1(b), power for the TM mode in HPWG is highly concentrated in the nano-fluidic channel. Therefore, the HPWG can also be used to achieve a detection limit lower than purely plasmonic sensors. For the last

application only the TM mode needs to utilized, but for the other sensors both TE and TM polarizations would be used.

3. Analysis and Optimization of the HPWG Sensor Performance

3.1. Method of Analysis and Figures of Merit

Choosing a proper figure of merit is critical for optimizing a biosensor design and also for comparison of different biosensors. A significant number of previous investigations of plasmonic sensors considered bulk and surface sensitivities defined in the previous section as figures of merit for the sensor. It is assumed that large bulk and surface sensitivities are indicative of a good biosensor. However, these assumptions are not always valid. Most biosensors are affinity type and a large bulk sensitivity is not an appropriate measure for evaluation of such sensors [15]. Although surface sensitivity is a more dependable quantity for an affinity sensor; a small surface sensitivity does not necessarily imply a small limit of detection (LoD) [16]. To overcome these difficulties Berini has defined the following figure of merit for surface sensing [16]

$$G = \frac{\left(\frac{\partial n_{\text{eff}}}{\partial a}\right)}{k_{\text{eff}}}. \tag{5}$$

The LoD for surface sensing was shown to be inversely proportional to G. Therefore, both surface sensitivity $(\partial n_{\text{eff}}/\partial a)$ and the imaginary part of effective mode index (k_{eff}) play equally important roles in determining LoD of a sensor. Surface sensitivity is directly proportional to field confinement. In general for any kind of plasmonic waveguide, there is a compromise between loss and confinement i.e., one can increase the mode confinement (with a corresponding increase in surface sensitivity) but this is always accompanied by an increase in propagation loss of the guided mode. Therefore surface sensitivity is not a true measure of LoD for an affinity sensor, and G should be used instead of surface sensitivity as the figure of merit for surface sensing. He has also defined a figure of merit for bulk sensing (H) and showed that LoD for bulk sensing is inversely proportional to H

$$H = \frac{\left(\frac{\partial n_{\text{eff}}}{\partial n_c}\right)}{k_{\text{eff}}}. \tag{6}$$

In this work, we investigate the applicability of HPWG sensor for affinity sensing and take large G as the criterion of a good biosensor.

For optimizing the sensor design it is important to understand the effects of various design parameters on the hybrid mode characteristics. The hybrid mode supported by HPWG is a combination of a dielectric waveguide mode and a SP mode. Changes in waveguide dimensions, material properties and wavelength of operation affect the two modes differently and therefore, the variations of the modal characteristics of the hybrid mode are also complicated and finding a general trend is challenging. To illustrate this, we have plotted the field profiles of the hybrid mode for three different silicon thicknesses (d) and for three different wavelengths in Fig. 3. The coordinate system used is the one shown in Fig. 1, i.e., $y = 0$ plane is the metal-nanochannel interface. For $d = 70$ nm, the guided mode always has hybrid nature and is highly confined in the nano-fluidic channel. For $d = 100$ nm the field profile is a combination of TM_0 mode supported by the silicon slab and the hybrid mode for 0.8 μm wavelength, and for longer wavelength, for example 1.4 μm, it becomes increasingly more confined in the nano-fluidic channel. For $d = 140$ nm, the field is very similar to TM_0 mode supported by a silicon slab for 0.8 μm wavelength [see Fig. 3(c)] and is highly confined in the nano-fluidic channel at a wavelength of 1.4 μm.

We conclude from the above investigation that the performance of the HPWG sensor has a complicated relationship with these parameters and a detailed numerical analysis is necessary to optimize the ultimate performance. We should point out that we have also investigated the

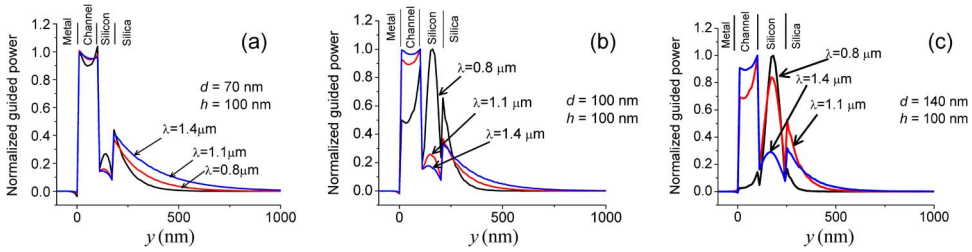

Fig. 3. Guided power intensity profiles for three different d at three different wavelengths $(\lambda = 0.8\ \mu\text{m}, 1\ \mu\text{m}, \text{ and } 1.4\ \mu\text{m})$ when the high index medium is silicon. (a) $d = 70$ nm, (b) $d = 100$ nm. (c) $d = 140$ nm. Channel thickness (h) is 100 nm in all cases.

effect of channel thickness on the sensor performance. Unlike the wavelength of operation and thickness of high index layer [d in Fig. 1(a)], there is a straightforward relation between the sensor performance and channel thickness. Irrespective of wavelength of operation and silicon thickness, decreasing the channel thickness always increases the mode confinement, and increases the magnitude of figure of merit for surface sensing (G). Therefore, we choose to fix the channel thickness during the optimization of our design.

The HPWG sensor can be used for two different types of applications. It can be used for single polarization measurements where only the TM mode is used to achieve a LoD lower than possible using a single interface SP sensor. It is also possible to use both the TE and TM polarizations to achieve an enhanced functionality, as described in Section 2. We optimized the HPWG sensor design for both types of applications. We concentrate our analysis to a one dimensional HPWG since accurate solutions for the guided modes of such a structure can be obtained analytically with little numerical effort. In addition, its mode characteristics e.g., field profiles, sensitivity, etc., closely resemble those of the more realistic two dimensional structure. A transfer matrix method is used to solve for the guided modes [16]. The permittivity of silica, silicon and gold are taken from [15] and spline interpolation was used to obtain the material properties at various wavelengths. The index of refraction of the liquid filling the nano-fluidic channel is assumed to be that of water. The material loss data of water has also been taken into account [16]. A spline interpolation was used to obtain all the material data at wavelengths of interest. The adlayer is assumed to be a homogenous, isotropic and uniform material having a wavelength independent relative permittivity of 1.5 [14]. Although fabrication and fluid flow through a channel of few tens of nanometer width have been experimentally demonstrated [17], a 100 nm channel thickness is chosen in this work for ease of implementation. The results of the analysis obtained from the analysis will serve as a guideline for designing two dimensional sensors similar to the one described in [9], which would not require the implementation of any nano-fluidic channel. For each of the two cases we vary the high index slab thickness and wavelength of operation to optimize G. The design parameters for both optimizations are chosen to ensure single mode operation. The highest value of G achievable from single interface plasmonic sensor $(G_{SP\_\max})$ is 0.28/nm and the corresponding value of H is 339/RIU [16]. These values are used as bench marks for evaluating the HPWG sensor performance. The choice of high index medium is not optimized in this work. Instead two different choices of high index medium (silicon and silicon nitride) are considered. Although we have carried out detail analysis of the effects of wavelength, channel thickness and high index layer thickness in our work, to keep the discussion brief, results from a selected number of cases are reported here, which should give the reader sufficient insight regarding the effects of various design parameters on sensor performance. The summary of optimized designs are presented in Tables 1 and 2.

3.2. Optimization for Single Polarization Operation

Since the TM mode is highly concentrated in the nanofluidic channel (see Fig. 1), it always has a higher sensitivity and larger G value than the TE mode. Therefore, for single polarization

TABLE 1

Optimization of the HPWG sensor for single polarization operation

High index material	d(nm)	G (nm^{-1})	H(/RIU)	λ (μm)	L_{Prop} (μm)
Silicon	155	0.545	208	1.1	81
Silicon nitride	250	0.396	102	0.85	47

TABLE 2

Optimization of the HPWG sensor for dual polarization operation

High index material	d (nm)	G^{TM} (nm^{-1})	H^{TM} (/RIU)	λ^{TM} (μm)	L^{TM}_{Prop} (μm)	G^{TE} (nm^{-1})	H^{TE} (/RIU)	λ^{TE} (μm)	L^{TE}_{Prop} (μm)
Silicon	170	0.597	200	1.05	90	0.012	41	1.1	280
Silicon nitride	100	0.31	120	1.1	37	0.0395	65	0.65	87

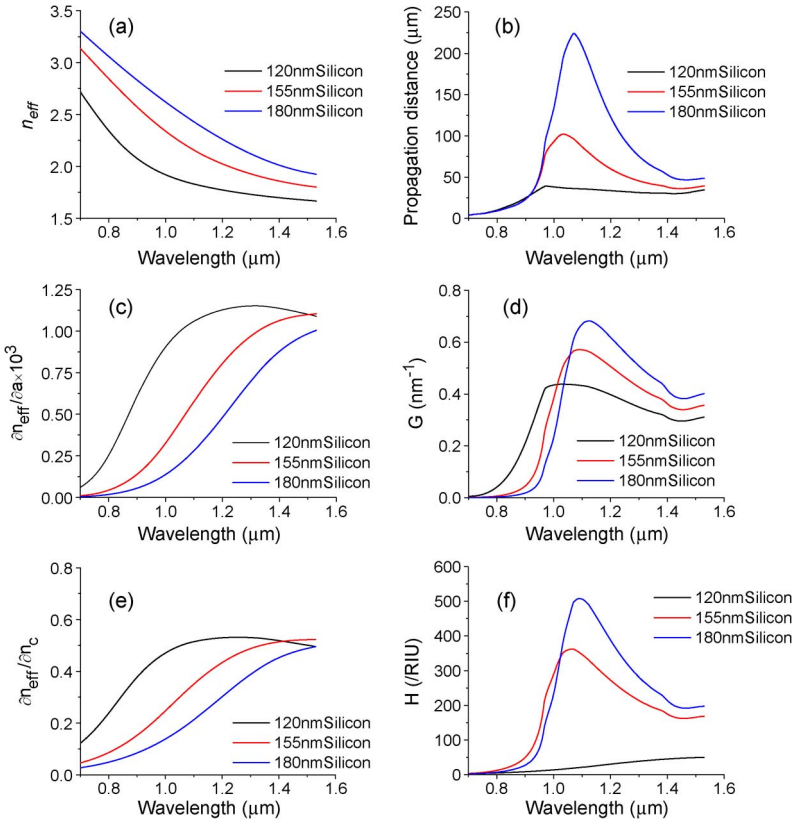

Fig. 4. Mode characteristics and sensing parameters of the TM mode for a HPWG in MZI configuration. Channel thickness is 100 nm, and the high index medium is silicon. (a) Effective mode index. (b) Propagation distance. (c) Surface sensitivity. (d) Figure of merit for surface sensing. (e) Bulk sensitivity. (f) Figure of merit for bulk sensing.

operation, we aim to maximize the G value for the TM mode while disregarding the TE mode. Fig. 4 shows the variations of the mode characteristics and sensing parameters as a function of wavelength for a number of different silicon thicknesses. Here propagation distance is defined as the distance over which power of the guided mode drops to 1/e of its initial magnitude. The

situation for these figures is close to the plots Fig. 3(b) and (c), i.e., for small channel thickness the mode is more dielectric mode like but for longer wavelength, the mode is concentrated more in the space region and becomes more hybrid in nature. As a result the propagation distance of the mode is longest for an intermediate wavelength, which depends on the silicon thickness. Since the mode is more confined in the nano-fluidic channel for longer wavelengths, the bulk and surface sensitivities also increase. This is in contrast to single interface SP mode for which both bulk and surface sensitivities monotonically decrease with increasing wavelength of operation. However, both G and H are largest for specific wavelengths, which do not correspond to maximum bulk or surface sensitivity in either of these cases. The G value obtained in the case of silicon nitride is less than silicon. To keep the discussion brief, we have not reported the details for silicon nitride here.

Table 1 summarizes the results of the optimization for single polarization operation. In the case of silicon slab the highest G value achievable is 0.545, which is 1.95 times that of (G_{SP_max}). Higher values of G are achievable for thicker silicon films. For $d = 300$ nm, G is 1.006 which is 3.5 time that of (G_{SP_max}). In this case, the guide becomes multimode which may not be convenient for sensing in MZI configuration, but can be useful in other configuration, for example prism coupling, where a mode is selectively excited by adjusting the angle of incidence. Since the index contrast between silicon nitride and water is relatively smaller, enhancement of power concentration in the channel is lower and hence in case of silicon nitride the value of G is closer to (G_{SP_max}).

Although the sensor performance for single polarization operation is optimum for 1.1 μm wavelength, one may prefer to design a sensor at 1.31 μm wavelength since commercial lasers are readily available at this wavelength. We also optimized the high index layer thickness for this wavelength. We found that for this wavelength the sensor performance is optimum for 170 nm thick silicon layer, and the value of G is 0.45, which is comparable to that mentioned for the optimum design at 1.1 μm.

3.3. Optimization for Dual Polarization Operation

In this case, the target of the optimization is to achieve large G values for both polarizations. Since the TE mode has a significantly lower sensitivity, for these applications we aim at maximizing G for the TE mode. Table 2 summarizes the results of optimization for dual polarization operation. To avoid ambiguity, the type of polarization is mentioned as superscript. For example G^{TM} is the highest G value expected for the TM polarization and the corresponding wavelength and the propagation distance are designated as λ^{TM} and L^{TM}_{Prop} respectively. A similar nomenclature is also used for the TE mode. When the high index medium is silicon, G^{TE} is 0.012 nm^{-1}, which is only 4.3% of G_{SP_max}. G^{TE} is significantly larger when the high index medium is silicon nitride instead of silicon. In this case for $d = 100$ nm, G^{TE} is more than 14% of G_{SP_max} while $G^{TM} = 0.31$ nm^{-1} which is slightly higher than G_{SP_max}. Since the results are better for silicon nitride than silicon, we plot the mode characteristics only for the silicon nitride case here. Fig. 5 shows the modal characteristics and sensing parameters for various silicon nitride thicknesses for the TM mode. In contrast to the case of Fig. 4, in this case the propagation distance monotonously increases with wavelength [see Fig. 5(b)]. Also both the surface and bulk sensitivities decrease with increasing wavelength [see Fig. 5(c) and (e)].

The wavelength of commercially available Helium-Neon laser is very close to that necessary for optimum sensor performance for the TE polarization operation (last row of Table 2). For the TM polarization the optimum performance is achieved for 1.1 μm wavelength, but one may prefer to use more readily available lasers of wavelength 1.31 μm. This would reduce the G by 25% but the G is still of comparable to that mentioned in Table 2 i.e., 0.0395. Fig. 6 shows the modal characteristics and sensing parameters for the TE mode for a number of silicon nitride thicknesses. In this case unlike the hybrid TM mode, power is concentrated in the silicon nitride region. As a result the mode is little affected by the presence of metal and the propagation distance is large. However, since the power is not highly concentrated in the nano-fluidic channel,

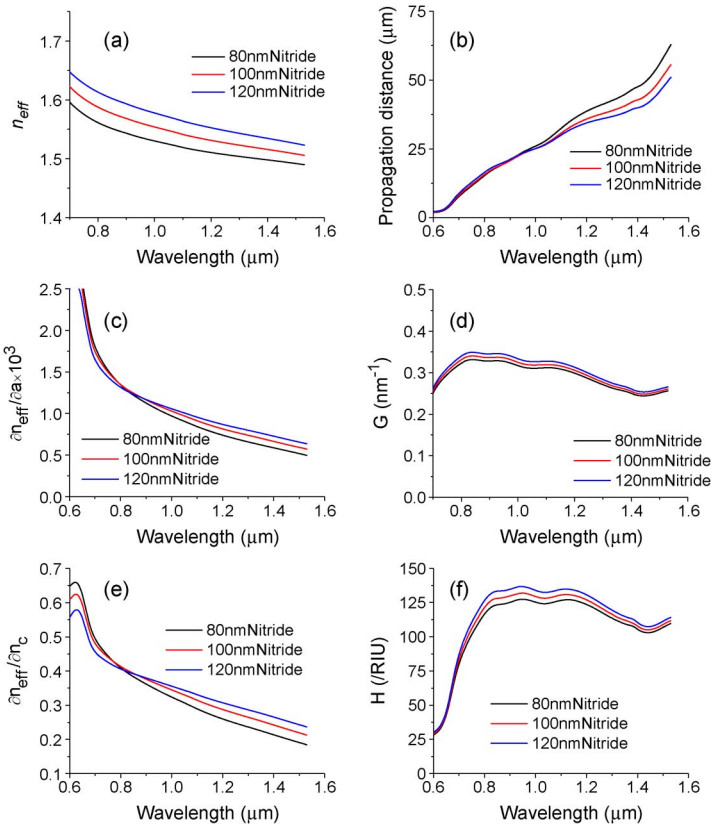

Fig. 5. Mode characteristics and sensing parameters of the TM mode for a HPWG in MZI configuration. Channel thickness is 100 nm, and the high index medium is silicon nitride. (a) Effective mode index. (b) Propagation distance. (c) Surface sensitivity. (d) Figure of merit for surface sensing. (e) Bulk sensitivity. (f) Figure of merit for bulk sensing.

the surface sensitivity is also low. The combination of low surface sensitivity [see Fig. 6(c)] and large propagation distance [see Fig. 6(b)] results in relatively smaller G than the TM mode.

The G value is valid as a figure of merit for the sensor only when the sensor length equals the propagation distance of the guided mode [16]. As shown in Table 2, the propagation distance of the TE and TM modes for the optimized design with silicon nitride as the high index layer are 87 μm and 37 μm, respectively. Therefore, it is not possible to simultaneously achieve $G^{TM} = 0.31$ nm^{-1} and $G^{TE} = 0.0395$ nm^{-1} for the same device length and a compromise must be made. We have extended Berini's work and defined an effective figure of merit for surface sensing (G_{eff}) with an arbitrary sensor length [18]

$$G_{eff} = \frac{x}{e^{(x-1)}} \times G. \tag{7}$$

Here, $x = L_{prop}/L$; L_{prop} and L are the propagation distance of the guided mode and length of sensing section respectively. G_{eff} is inversely proportional to LoD for arbitrary sensor length L. In case of the design presented in Table 2, for $L = 65$ μm, we achieve $G_{eff}^{TM} = 0.91 G_{SP\_max}$ and $G_{eff}^{TM} = 0.127 G_{SP\_max}$. We take this as a reasonable compromise between the performances achieved for TE and TM modes.

4. Discussions and Conclusion

In this work, we have examined the HPWG sensor in detail and optimized it for both single and dual polarization operations. Here we summarize the important conclusions reached from this analysis. A number of previous reports on HPWG sensor investigated the performance of the

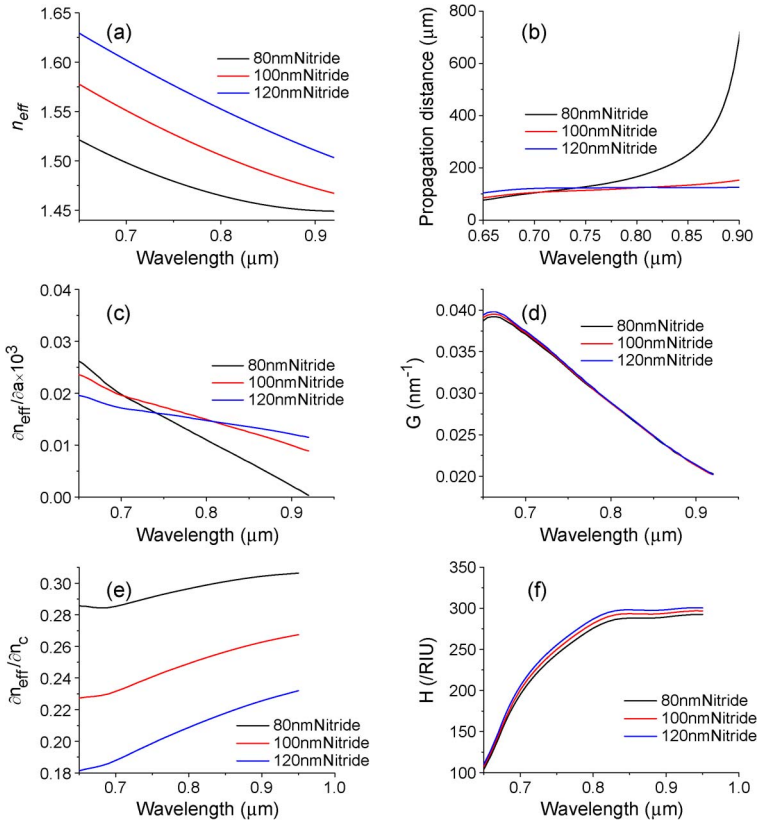

Fig. 6. Mode characteristics and sensing parameters of the TE mode for a HPWG in MZI configuration. Channel thickness is 100 nm, and the high index medium is silicon nitride. (a) Effective mode index. (b) Propagation distance. (c) Surface sensitivity. (d) Figure of merit for surface sensing. (e) Bulk sensitivity. (f) Figure for merit for bulk sensing.

HPWG sensor at a fixed wavelength of 1.55 μm [8], [9]. Our work shows that the optimum wavelengths for both single and dual polarization operations are significantly shorter than 1.55 μm. Therefore, the performance of the optimized HPWG sensor can be better than predicted in previous reports [7]–[9]. For single polarization operation silicon is a better choice than silicon nitride and the opposite is true for dual polarization operation. The sensor design is compatible with planar fabrication technology for both choices. For single polarization operation the best *G*-value for the HPWG sensor can be almost twice that of G_{SP_max}. Larger *G*-values can be achieved by using other plasmonic sensing schemes [16]. However the enhancement of *G* for those structures is accompanied by a corresponding increase of *H*. In contrast the *H* of the HPWG sensor is even smaller that that of single interface SP. The optimized HPWG sensor is therefore less susceptible to effect of change of bulk properties, which is useful for surface sensing. Plasmonic sensors are compact, very suitable for analysis of chemical kinetics but since they can support only TM modes, the information obtained from such sensing is limited. Dual polarization interferometry (DPI) can obtain structural information about biological molecules by utilizing both polarizations but its long length (more than 10 millimeters) makes it less suitable for investigation of initial chemical kinetics [19]. Moreover, the absence of a metal surface makes functionalization of DPI sensor surface challenging. The results of optimization presented in this work illustrate that for a HPWG sensor the sensitivity for both polarization is significant and therefore such a device combines the benefits of DPI (polarization diversity) and plasmonic sensing (compactness, ease of functionalization) on the same platform.

For the sake of simplicity and also to be able to compare the performance of the HPWG sensor with previously reported plasmonic sensors, we have analyzed a one dimensional structure

in this work. Implementation of the device can be considerably simplified by rotating the structure by 90 degree on the substrate, as explained in [9]. Detailed analysis of this two dimensional HPWG sensor will be reported in our future publications. The results presented in this work should be useful for design of MZI type biosensor using the HPWG. The results also provide valuable insight which may be useful for designing the HPWG sensor in other configurations.

References

[1] M. Z. Alam, J. Meier, J. S. Aitchison, and M. Mojahedi, "Super mode propagation in low index medium," presented at the 2007 Conf. Lasers Electro-Optics/Quantum Electronics Laser Sci., Baltimore, MD, USA, Paper ID: JThD112.

[2] M. Z. Alam, J. S. Aitchison, and M. Mojahedi, "A marriage of convenience: Hybridization of surface plasmon and dielectric waveguide modes," *Laser Photon. Rev.*, vol. 8, no. 3, pp. 394–408, May 2014.

[3] M. Z. Alam, J. Meier, J. S. Aitchison, and M. Mojahedi, "Propagation characteristics of hybrid modes supported by metal-low-high index waveguides and bends," *Opt. Exp.*, vol. 18, no. 12, pp. 12971–12979, Jun. 2010.

[4] M. Z. Alam, J. S. Aitchison, and M. Mojahedi, "Compact and silicon-on-insulator compatible hybrid plasmonic TE-pass polarizer," *Opt. Lett.*, vol. 37, no. 1, pp. 55–57, Jan. 2012.

[5] M. Z. Alam, J. S. Aitchison, and M. Mojahedi, "Polarization-independent hybrid plasmonic coupler for silicon-on-insulator platform," *Opt. Lett.*, vol. 37, no. 16, pp. 3417–3419, Aug. 2012.

[6] A. Joushaghani, B. A. Kruger, S. Paradis, J. S. Aitchison, and J. K. Poon, "Sub-volt broadband hybrid plasmonic-vanadium dioxide switches," *Appl. Phys. Lett.*, vol. 102, no. 6, pp. 061101, Feb. 2013.

[7] M-S. Kwon, "Theoretical investigation of an interferometer-type plasmonic biosensor using a metal-insulator-silicon waveguide," *Plasmonics 5*, vol. 5, no. 4, pp. 347–354, Dec. 2010.

[8] L. Zhou, X. Sun, X. Li, and J. Chen, "Miniature microring resonator based on a hybrid plasmon waveguide," *Sensors* vol. 11, no. 7, pp. 6856–6867, 2011.

[9] M. Z. Alam, S. Aitchison, and M. Mojahedi, "Vertical wall affinity sensor with polarization diversity," in *Opt. Sensors, OSA Tech. Dig., Opt. Soc. Amer.*, Toronto, ON, USA, 2011, paper SMB3.

[10] F. Bahrami, M. Z. Alam, J. S. Aitchison, and M. Mojahedi, "Dual polarization measurements in the hybrid plasmonic biosensors," *Plasmonics*, vol. 8, no. 2, pp. 465–473, Jun. 2013.

[11] E. D. Palik, *Handbook of Optical Constants of Solids*. New York, NY, USA: Academic, 1985.

[12] L. Kou, D. Labrie, and P. Chylek, "Refractive indices of water and ice in the 0.65- to 2.5-μm spectral range," *Appl. Opt.*, vol. 32, no. 19, pp. 3531–3540, Jul. 1993.

[13] N. Freeman, *Proteins at Solid-Liquid Interfaces—Principles and Practice, Part II*. New York, NY, USA: Springer-Verlag, 2006, pp. 75–104, Ch. 4.

[14] K. Tiefenthaler and W. Lukosz, "Sensitivity of grating couplers as integrated-optical chemical sensors," *J. Opt. Soc. Amer. B*, vol. 6, no. 2, pp. 209–220, Feb. 1989.

[15] S. Janz *et al.*, *Advanced Photonic Structures for Biological and Chemical Detection*. New York, NY, USA: Springer-Verlag, 2009, Ch. 9.

[16] P. Berini, "Bulk and surface sensitivities of surface plasmon waveguides," *New J. Phys.* vol. 10, no. 10, pp. 105010-1–105010-37, 2008.

[17] X. Liang, K. J. Morton, R. H. Austin, and S. Y. Chou, "Single sub-20 nm wide, centimeter long nanofluidic channel fabricated by novel nanoimprint mold fabrication and direct imprinting," *Nano Lett.* vol. 7, no. 12, pp. 3774–3780, 2007.

[18] M. Z. Alam, "Hybrid plasmonic waveguides: Theory and applications," Ph.D. dissertation, Univ. Toronto, Toronto, ON, Canada, 2012. [Online]. Available: https://tspace.library.utoronto.ca/handle/1807/33902

[19] A. W. Sonesson, T. H. Callisen, H. Brismar, and U. M. Elofsson, "A comparison between dual polarization interferometry (DPI) and surface plasmon resonance (SPR) for protein adsorption studies," *Colloids Surfaces B: Biointerfaces*, vol. 54, no. 2, pp. 236–240, 2006.